

Stability of the Martian atmosphere: Is heterogeneous catalysis essential?

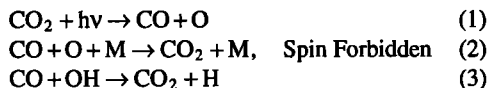
Sushil K. Atreya and Zhen Gang Gu

Department of Atmospheric, Oceanic and Space Sciences, University of Michigan, Ann Arbor

Abstract. A comprehensive homogeneous gas phase photochemical model is developed to study the problem of stability of the Martian atmosphere. The one-dimensional model extends from the ground up to 220 km, passing through the homopause at 125 km. The model thus couples the lower (neutral) atmosphere to the ionosphere above which provides significant downward flux of carbon monoxide and oxygen atoms. It is concluded on the basis of currently accepted values for globally and seasonally averaged water vapor abundance, dust opacity and the middle atmospheric eddy mixing coefficient, as well as the relevant laboratory data (particularly the temperature dependence of CO₂ absorption cross section and the rate constant for CO + OH reaction), that the rate of re-formation of carbon dioxide exceeds its photolytic destruction rate by about 40%. Furthermore, it is found that this result is virtually independent of the choice of eddy mixing coefficient, unless its value in the middle atmosphere exceeds 10⁸ cm²s⁻¹ or is far smaller than 10⁵ cm²s⁻¹, or the dust opacity, unless it exceeds unity, or the water vapor mixing ratio at the surface, unless it is far smaller (≤1 ppm) or far greater (≥500 ppm) than the average value (~150 ppm). Since none of these extremes represent globally and seasonally averaged conditions on Mars, we propose that the present model requires existence of a mechanism to throttle down the recycling rate of carbon dioxide on Mars. Therefore, it is suggested that a heterogeneous process which provides a sink to the species that participate in the recycling of CO₂, i.e., H₂O, H₂O₂, OH, CO or O, in particular, may be necessary to bring about the balance between the CO₂ recycling rate and its photolytic destruction rate. Aerosols of dust or ice (pure or doped water or carbon dioxide ice present in the atmosphere of Mars) can provide the appropriate adsorption sites for the above heterogeneous process. Despite our conclusion that some heterogeneous process may be needed, it is important to recognize that one-dimensional models can only provide first-order results which, most likely, represent globally and seasonally averaged conditions. However, it is only after actual temporal, latitudinal and longitudinal variations of relevant atmospheric parameters are included in the model that one can determine fully whether the problem of atmospheric stability still continues to persist and whether some heterogeneous process is required to correct it.

Introduction

The classical problem of the stability of Martian atmosphere is revisited in view of improved planetary and laboratory data. Nearly two decades ago, recognizing that once photodissociated, the Martian CO₂ cannot be reconstituted by the reverse reaction of its products since the reaction is spin forbidden, *McElroy and Donahue* [1972] and *Parkinson and Hunten* [1972] proposed oxidation of CO to CO₂ by a process that involves catalysis by the hydroxyl radicals. The relevant reactions are as follows:

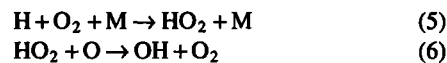


(where M represents the background gas).

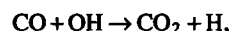
In the absence of recycling, CO₂ in the Martian atmosphere would have been irreversibly converted to CO and O₂ in less than 6000 years, the latter being formed in the following three-body recombination reaction:



It is known, however, that the level of CO₂ in the Martian atmosphere is stable except for regular, seasonal variations of approximately 30% due to the CO₂ deposition on and reevaporation from the polar ice caps. Moreover, the present atmospheric levels of O₂ and CO, which are approximately 0.12% and 0.07%, respectively, do not continue to build up, despite the fact that these levels would have been attained in less than 6 years. Evidently some effective mechanism for recycling CO₂ while at the same time maintaining the levels of O₂ and CO is operative on Mars. The hydroxyl catalysis mechanism of *McElroy and Donahue* [1972] (MD, hereafter) and *Parkinson and Hunten* [1972] (PH, hereafter) require a source of OH, which is ultimately in the Martian water vapor; but the two models differ significantly in details. In the MD model, the source of OH is in HO₂, and the scheme is as follows:



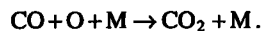
And, combined with



Copyright 1994 by the American Geophysical Union.

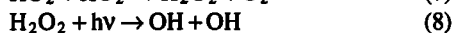
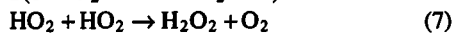
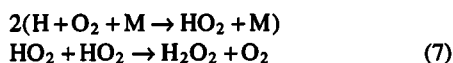
Paper number 94JE01085.
0148-0227/94/94JE-01085\$05.00

the net result is

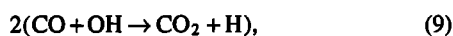


The MD model required an eddy diffusion coefficient, K , exceeding $10^8 \text{ cm}^2 \text{ s}^{-1}$ in the middle atmosphere (25–45 km), which is now found to be an unacceptably high value for this region. Such high values of K were needed to prevent the buildup of an excessive amount of oxygen atoms in the upper atmosphere, and to rapidly transport CO to the lower atmosphere, where its reaction with the hydroxyl radical would result in the formation of CO_2 .

The above difficulty regarding K in the MD model was largely alleviated in the PH model, in which an additional large source of OH from hydrogen peroxide (H_2O_2) was considered. The PH model assumed $K = 5 \times 10^6 \text{ cm}^2 \text{ s}^{-1}$ in the middle atmosphere; however, the “average” water vapor mixing ratio required in this model must be of the order of 500 ppm in order to balance the loss and production rates of CO_2 . The relevant set of reactions in the PH model is given below:



And, combined with



the net result is



The PH model thus effectively recycles CO_2 without having to resort to unreasonably large values of K in the middle atmosphere. The difficulty, however, is with the assumption of a nearly “wet” atmosphere. Although the amount of water vapor on Mars varies from less than 1 pr μm (1 pr $\mu\text{m} = 10^{-4} \text{ g cm}^{-2}$

$\text{H}_2\text{O} = 3.35 \times 10^{18} \text{ molecules cm}^{-2}$ H_2O ; 1 pr $\mu\text{m} \sim 15 \text{ ppm}$ for uniformly mixed H_2O) in early spring to 60–70 pr μm in the summer [Farmer *et al.*, 1977], the globally and seasonally averaged value is in the 10–15 pr μm range or 150–225 ppm [Jakosky and Farmer, 1982], which is far below that required in the PH model.

A variation on the PH and MD models by Kong and McElroy [1977] (KM, hereafter) considered the possibility of an active surface, but it also required unacceptably high values of K in the middle atmosphere (once improved laboratory kinetic data are taken into account as discussed by Treya and Blamont [1990]).

In view of the above difficulties with the previous models, Treya and Blamont [1990] suggested that the recombination of CO and O to recycle CO_2 could be facilitated by heterogeneous processes in the atmosphere of Mars through catalysis on the surfaces of aerosols of dust or ice, either directly or on chemical reactions. In part, this suggestion was prompted by laboratory measurements which indicated that in the presence of long-wavelength sunlight in the 210–390 nm range, oxidation of CO to CO_2 by O can occur if catalyzed by anatase (titanium oxide, TiO_2 ; [Thevenet *et al.*, 1974]). The Martian surface contains 0.5–1% TiO_2 , and presumably it is also present in the airborne dust. Laboratory data on the accommodation coefficients of CO and O on pure ice, and a small number of minerals found in the Martian surface (magnetite, hematite, anatase, etc.) indicated that the largest value is for TiO_2 [Leu *et al.*, 1992]. Even for TiO_2 , however, the accommodation coefficient is only 10^{-4} , which is

Table 1. Chemical Reactions in the Neutral Atmosphere Important for the Atmospheric Stability Problem

Reactions	Rate Constants ^a	References
R1	$\text{H}_2\text{O} + h\nu \rightarrow \text{OH} + \text{H}$	Thompson <i>et al.</i> [1963] for $\sigma_{\text{H}_2\text{O}}$
R2	$\text{CO}_2 + h\nu \rightarrow \text{CO} + \text{O}$	see text for σ_{CO_2}
R3	$\text{CO} + \text{O} + \text{M} \rightarrow \text{CO}_2 + \text{M}$	Slanger <i>et al.</i> [1972]
R4	$\text{H} + \text{O}_2 + \text{M} \rightarrow \text{HO}_2 + \text{M}$	DeMore <i>et al.</i> [1992]
R5	$\text{HO}_2 + \text{HO}_2 \rightarrow \text{H}_2\text{O}_2 + \text{O}_2$	DeMore <i>et al.</i> [1992]
R6	$\text{O} + \text{HO}_2 \rightarrow \text{OH} + \text{O}_2$	Atkinson <i>et al.</i> [1989]
R7	$\text{H}_2\text{O}_2 + h\nu \rightarrow \text{OH}$	Okabe [1978] for $\sigma_{\text{H}_2\text{O}_2}$
R8	$\text{HO}_2 + h\nu \rightarrow \text{OH} + \text{O}$	Okabe [1978] for σ_{HO_2}
R9	$\text{CO} + \text{OH} \rightarrow \text{CO}_2 + \text{H}$	Larson <i>et al.</i> [1988]
R10	$\text{H} + \text{HO}_2 \rightarrow 2\text{OH}$	Atkinson <i>et al.</i> [1989]
R11	$\text{H} + \text{HO}_2 \rightarrow \text{H}_2 + \text{O}_2$	Atkinson <i>et al.</i> [1989]
R12	$\text{H} + \text{HO}_2 \rightarrow \text{H}_2\text{O} + \text{O}$	Atkinson <i>et al.</i> [1989]
R13	$\text{H} + \text{O}_3 \rightarrow \text{OH} + \text{O}_2$	DeMore <i>et al.</i> [1992]
R14	$\text{O} + \text{OH} \rightarrow \text{O}_2 + \text{H}$	DeMore <i>et al.</i> [1992]
R15	$\text{O} + \text{O} + \text{M} \rightarrow \text{O}_2 + \text{M}$	Tsang and Hampson [1986]
R16	$\text{O} + \text{O}_2 + \text{M} \rightarrow \text{O}_3 + \text{M}$	DeMore <i>et al.</i> [1992]
R17	$\text{OH} + \text{HO}_2 \rightarrow \text{H}_2\text{O} + \text{O}_2$	Keyser [1988]
R18	$\text{H}_2\text{O}_2 + \text{OH} \rightarrow \text{HO}_2 + \text{H}_2\text{O}$	DeMore <i>et al.</i> [1992]
R19	$\text{O}_3 + h\nu \rightarrow \text{O}_2 + \text{O}(^1\text{D})$	WMO [1985] for σ_{O_3}
R20	$\text{O}_3 + h\nu \rightarrow \text{O}_2 + \text{O}(^3\text{P})$	WMO [1985] for σ_{O_3}
R21	$\text{O}_2 + h\nu \rightarrow 2\text{O}$	Watanabe <i>et al.</i> [1953]
R22	$\text{O}(^1\text{D}) + \text{H}_2\text{O} \rightarrow 2\text{OH}$	DeMore <i>et al.</i> [1992]
R23	$\text{O}(^1\text{D}) + \text{CO}_2 \rightarrow \text{O} + \text{CO}_2$	Shi and Barker [1990]
R24	$\text{O}(^1\text{D}) + \text{H}_2 \rightarrow \text{OH} + \text{H}$	Gericke and Comes [1981]

^a The units for rate constants are $\text{cm}^3 \text{ s}^{-1}$ for two-body reactions and $\text{cm}^6 \text{ s}^{-1}$ for three-body reactions. NIST Chemical Kinetics Database (version 5.0) was also consulted in choosing the rate constants. M represents the background gas, CO_2 .

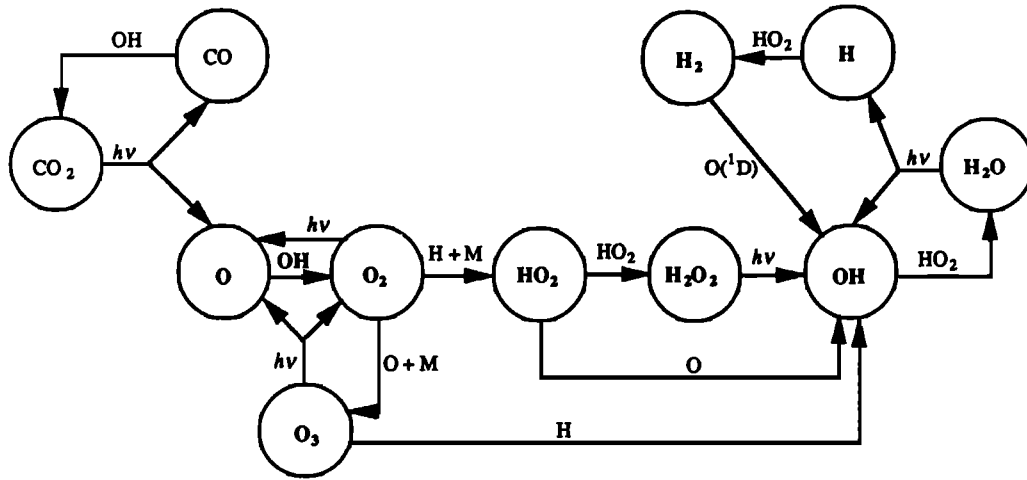


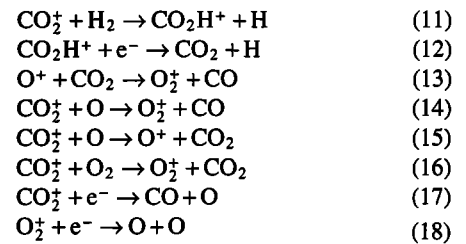
Figure 1. Scheme of chemical reactions in the neutral atmosphere important for the stability problem.

not too promising for recycling CO₂ by the above heterogeneous process. Although all of the relevant accommodation coefficients have not yet been measured, in view of the new information on the relevant planetary parameters and laboratory data, it is important to carry out a complete photochemical modeling calculation to reevaluate the necessity and role of heterogeneous processes in the problem of Martian atmospheric stability.

In this paper we present a comprehensive one-dimensional photochemical model of the atmosphere of Mars which explicitly couples the lower neutral atmosphere with the ionosphere; inclusion of the latter is important since additional fluxes of carbon monoxide and oxygen are produced in the ionosphere. (D.M. Hunten (personal communication, 1993) has pointed out that flux of neutrals from the ionosphere was considered in the PH model also even though the model was restricted to low-middle neutral atmosphere.) The present model also takes into consideration the latest laboratory measurements of the relevant rate constants and cross sections along with their temperature dependence. Furthermore, measurements of eddy diffusion coefficients in the middle atmosphere have become available as a result of the recent analyses of solar occultation observations from Phobos [Chassefiere *et al.*, 1992] and of the water vapor haze distribution from Viking Orbiters [Kahn, 1990].

The Photochemical Model

The homogeneous gas phase photochemical model of this paper ranges from the surface up to 220 km, passing through the homopause at approximately 125 km. The significant chemical reactions in the neutral atmosphere relevant for the atmospheric stability problem are listed in Table 1 and are illustrated schematically in Figure 1. Attention is directed to the reactions leading up to the formation and subsequent loss of the hydroxyl radical, OH, since OH is expected to play a crucial role in the stability of CO₂, O₂ and CO in the Martian atmosphere. As we will see later, reaction R6 (Table 1) is the dominant contributor to the OH produced, with significant contribution from reaction R7, while reactions R8, R10 and R13 contribute far less. The reactions in the top left and the right sides of Figure 1 show the ultimate fate of OH produced above. In particular, loss via reaction R9 leads to the formation of CO₂. The following basic ionospheric reactions relevant to the production of carbon monoxide and oxygen have been included in the model.



Due to the much higher density of carbon dioxide, solar flux produces more CO₂⁺ than any other ions. However, most of the CO₂⁺ ions are converted to O₂⁺ rapidly through above reactions 14 and 16.

A vast majority of the rate constants, and, where applicable, their temperature and pressure dependence, have been revised compared to the values used in MD, PH and KM models. Particularly noteworthy is the change in the rate constant for the principal pathway for recycling CO₂ (R9, Table 1). The latest laboratory measurements give a value which is nearly constant with temperature, unlike the old value which was highly temperature dependent and smaller. This is clearly illustrated in Figure 2 for the temperature profile used here. In the region critical for the recycling of CO₂, 20-50 km, the old rate constant is a factor of 3-7 smaller than the present measurement; the new rate constant will thus result in a greater recycling rate for CO₂.

The choice of the photoabsorption cross sections, σ, of CO₂ and H₂O could also have significant impact on the balance between photolysis loss and the recycling of CO₂. With regard to σ_{CO₂}, there are two important considerations: temperature dependence of the cross sections, and the relative importance of Rayleigh scattering in the Martian atmosphere in the wavelength region of the CO₂ photoabsorption. Three curves are shown in Figure 3: extinction cross sections of CO₂ at room temperature (298 K) from Shemansky [1972], which combine absorption and Rayleigh scattering; CO₂ absorption cross sections at 200 K from Lewis and Carver [1983]; and the Rayleigh scattering cross sections σ_R, which are calculated using the following relationship:

$$\sigma_R = 8\pi/3[(2\pi/\lambda)^4 \alpha^2 d] \quad (19)$$

where λ is the wavelength of radiation being scattered by molecules whose average dielectric polarizability is

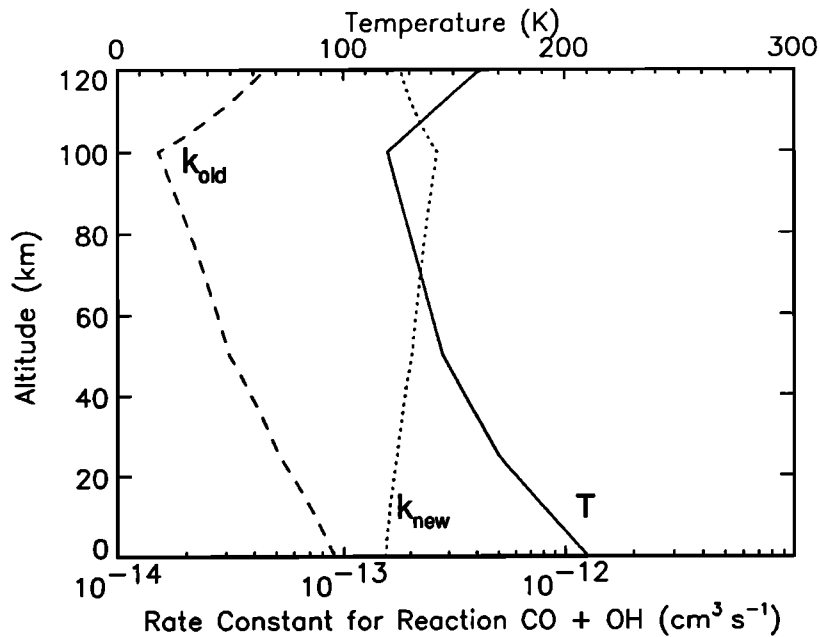


Figure 2. The old and the new rate constants for the $\text{CO} + \text{OH} \rightarrow \text{CO}_2 + \text{H}$ reaction versus the assumed temperature profile. Parameters k_{old} and k_{new} are equal to $9 \times 10^{-13} \exp(-500/T)$ and $4.35 \times 10^{-14} (T/298)^{1.35} \exp(365/T)$, respectively.

$\alpha(2.911 \times 10^{-24} \text{ cm}^3 \text{ for CO}_2)$, and d is the depolarization factor [Heddle, 1962],

$$d = (6 + 3\rho_n) / (6 - 7\rho_n). \quad (20)$$

With the normal depolarization ratio, $\rho_n = 0.0774$ for CO_2 [Shemansky, 1972], the depolarization factor d becomes 1.14. Thus the Rayleigh scattering cross sections for CO_2 are about 14% greater with this factor included.

From Figure 3 it is apparent that, for CO_2 , Rayleigh scattering begins to be comparable to photoabsorption at around 200 nm, while it almost completely dominates beyond 204 nm. It is also

evident from Figure 3 that the inclusion of temperature dependence of CO_2 cross sections is very important, since the cross sections are reduced by a factor of 2-3 at 200 K compared to those at room temperature. Since the globally averaged model of this paper corresponds to a temperature closer to 200 K for the surface, lower, and the middle atmospheres of Mars, the CO_2 absorption cross sections at 200 K are used. The temperature dependent cross sections have, however, been measured only up to 197 nm [Lewis and Carver, 1983]. To obtain the values at 200 K beyond this wavelength, Rayleigh scattering cross sections are subtracted from Shemansky's extinction cross sections, and the result is divided by a factor of 2 to be consistent with the temper-

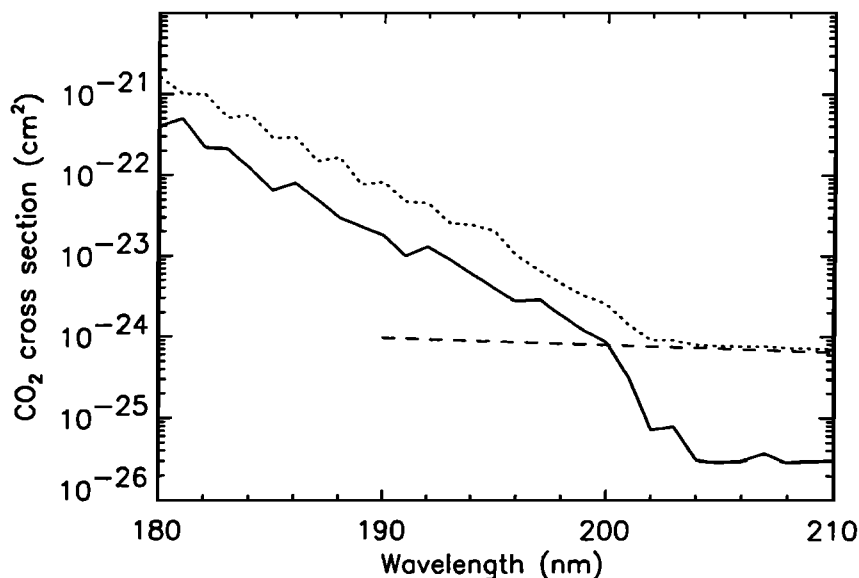


Figure 3. Extinction cross sections [Shemansky, 1972] (dotted line) at room temperature, absorption cross sections at 200 K [Lewis and Carver, 1983] (solid line), and the Rayleigh scattering cross sections (dashed line) of CO_2 .

ature dependent behavior at wavelengths below and in the vicinity of 197 nm. To be sure, although Rayleigh scattering cross sections are subtracted systematically from the extinction cross sections, they are included in the calculation of the solar flux available at a given altitude. An obvious impact of the use of new CO₂ absorption cross sections which are smaller by a factor of 2 to 3 compared to those used in the previous above mentioned models, is that the CO₂ photolysis rate would be correspondingly lower. With the loss rate of CO₂ being smaller, and the production rate greater (due to greater k for R9 (Table 1); discussion above), the production to loss ratio of CO₂ would be much greater in the previous models if all other parameters were unchanged. We will discuss this point more specifically in the context of a previous model a little later, but here it would suffice to note that the new laboratory data would exert a significant control over the stability of the Martian atmosphere. Previously, *Anbar et al.* [1993a] also suggested that inclusion of temperature dependence in σ_{CO_2} could minimize or even reverse the sense of CO₂ stability problem.

The situation with the H₂O absorption cross section is less satisfactory. The measurements are available to a good accuracy up to 189 nm at room temperature only [*DeMore et al.*, 1992; *Hudson and Keiffer*, 1975]. *Thompson et al.*'s [1963] measurements extend the range to 198 nm; however, they are less reliable beyond 189 nm. It is not apparent whether a temperature dependence similar to that of the CO₂ absorption cross sections discussed above (quite large), or that of O₃ (negligible) will be valid for H₂O. In the model given in this paper, sensitivity of the atmospheric stability to the possible temperature dependence of the H₂O absorption cross section is studied. Since H₂O cross sections directly affect the OH production rate, there could be a notable change in the CO₂ production to loss ratio if the H₂O cross sections at low temperatures turned out to be significantly different than the room temperature values.

The solar fluxes are taken from a Solar Maximum Explorer (SME) database for 1983/March conditions. In fact, the values are deceptively similar to those given by *Mount and Rottman* [1983] for the 1982/May period. The solar fluxes were divided by a factor of 2 to obtain diurnal averages; they were further reduced by the Cos 60° factor to obtain seasonal average values. For the nominal model, a mean vertical optical depth of 0.4 in the ultraviolet at the ground [*Krasnopolsky*, 1993] is assumed for the dust. The dust is taken to be well mixed with the atmospheric gases, which is a reasonably good assumption up to the altitudes of importance for the atmospheric stability question. The optical depth of dust in the atmosphere of Mars can vary dramatically, exceeding 2 (in the red-infrared) during the great dust storms such as those in the southern hemisphere summers [*Zurek*, 1982]. Even under "clear" conditions, the value rarely drops below 0.2 in the red-infrared [*Zurek*, 1982; *Drossart et al.*, 1991]. The sensitivity of results to the optical depth of dust will be discussed.

The Viking observations indicated that the homopause on Mars is located approximately 125 km above the surface, where the atmospheric density is $4 \times 10^{10} \text{ cm}^{-3}$ and the eddy diffusion coefficient is $10^8 \text{ cm}^2 \text{ s}^{-1}$ [*Nier and McElroy*, 1977]. For the problem of atmospheric stability, however, the relevant atmospheric region is below approximately 50 km. Although the results are far from convergence, a consensus is beginning to emerge from the analyses of dust profiles observed from Phobos [*Korablev et al.*, 1991; *Chassefiere et al.*, 1992], and water vapor haze layers observed from Phobos [*Chassefiere et al.*, 1992] and Viking [*Kahn*, 1990] spacecrafts. *Krasnopolsky* [1993] has compiled a profile of eddy diffusion coefficients based on these data.

A value of the order of $10^6 \text{ cm}^2 \text{ s}^{-1}$ up to 40 km, with an uncertainty of a factor of 3 to 5 is now generally accepted. Between 40 km and 80 km the value rises linearly to $10^7 \text{ cm}^2 \text{ s}^{-1}$. It then stays constant at $10^7 \text{ cm}^2 \text{ s}^{-1}$ up to 100 km, and a variation with atmospheric density, n , analogous to that in the Earth's atmosphere, i.e., $K \propto n^{-0.5}$ [*Lindzen*, 1971, 1981; *Hunten*, 1975] is assumed beyond 100-km altitude. Although molecular diffusion of species is considered from the ground up in our model, it only dominates beyond the homopause. The molecular diffusion coefficients are given by the following expression

$$D = AT^s/n \quad (21)$$

[*Banks and Kockarts*, 1973], where T and n are atmospheric temperature and number density, respectively. For atomic hydrogen, $A = 8.4 \times 10^{17}$, $s = 0.597$; for molecular hydrogen, $A = 2.23 \times 10^{17}$, $s = 0.75$; for the rest of the neutral species, $A = 10^{17}$ and $s = 0.75$.

The surface and atmospheric temperatures on Mars show considerable seasonal variations. In our nominal model, a mean temperature profile taken from *Seiff* [1982] is used. Water vapor and hydrogen peroxide are the two constituents which can undergo condensation on Mars (CO₂ does not condense at temperatures in the nominal model, but it is not a priori ruled out for other thermal profiles). The saturation values of H₂O and H₂O₂ are given by the following expressions:

$$\log_{10} V_{\text{H}_2\text{O}} = -2445.5646/T + 8.23121 \log_{10} T \\ -0.01677006T + 1.20514 \times 10^{-5} T^2 - 6.757169 \quad (22)$$

(for $173\text{K} \leq T \leq 273\text{K}$ [*Washburn*, 1924]), where $V_{\text{H}_2\text{O}}$ is the saturation vapor pressure of H₂O in mmHg, and T is temperature in °K,

$$n_{\text{H}_2\text{O}_2} = 2.7 \times 10^9 [\exp(T-180)/3.4] \quad (23)$$

$140\text{K} < T < 190\text{K}$ [*Krasnopolsky*, 1986], where $n_{\text{H}_2\text{O}_2}$ is the saturation number density of H₂O₂ in cm^{-3} . Water vapor begins to condense in the lower atmosphere; H₂O₂, however, does not condense much unless the atmosphere is considered to be wet, i.e., with H₂O exceeding 30 μm .

The photochemical model solves the coupled continuity and diffusion equations for 10 species: CO, O₂, H₂O, H₂, H₂O₂, O, H, OH, O₃ and HO₂. CO₂ is the background gas and its density is fixed. We use the Newton-Raphson technique [*Press et al.*, 1989] to iterate the finite differenced equations from the surface to 220 km, with a 1-km height resolution. The lower and upper boundary fluxes are taken to be zero.

Model Results

We have first attempted to reproduce the calculations of MD and PH models to test our numerical technique and to carry out an important sensitivity study on these previous models. To reproduce the earlier models, the input parameters, i.e., chemical reactions and the associated kinetics data, cross sections, solar fluxes, and atmospheric density, temperature and eddy mixing profiles, were taken to be identical to those in the MD and PH models. Figure 4 shows the results of calculations based on our numerical technique and the input parameters corresponding to the MD model. There is an excellent agreement between the density profiles calculated here and those given in Figure 2 of the MD paper, giving us confidence in our numerical method. In

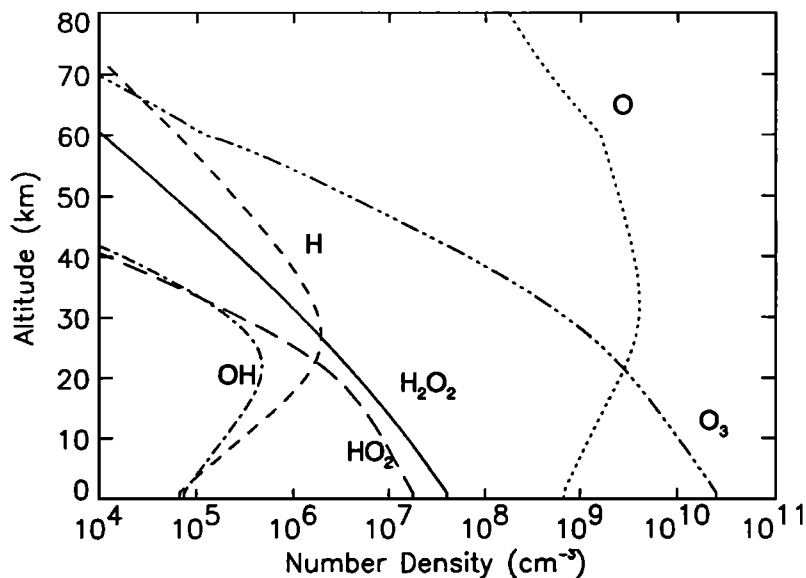


Figure 4. Distribution of species calculated for parameters and chemistry used in the MD model.

Figure 5 we present our calculations of the height-integrated loss rate due to photolysis, L , and production rate, P , of CO_2 for three assumed values of the eddy diffusion coefficient, which are taken constant with altitude as was done in the MD model. The values of P and L , and the ratio of P to L , which we term the atmospheric stability parameter, S_a , are listed in Table 2 ($S_a = 1$ for complete stability). It is apparent from Figure 5 and Table 2 that for an eddy diffusion coefficient of $1.5 \times 10^8 \text{ cm}^2 \text{ s}^{-1}$, the value adopted in the MD model, the loss rate of CO_2 is nearly balanced by its recycling rate. It is also clear that for $K = 1.5 \times 10^5$, or $1.5 \times 10^6 \text{ cm}^2 \text{ s}^{-1}$ the stability ratio falls far short of one; this is also implied in the discussion by MD of their model, although no explicit results for $K < 1.5 \times 10^8 \text{ cm}^2 \text{ s}^{-1}$ are presented there.

As mentioned earlier, values of K much greater than $10^6 \text{ cm}^2 \text{ s}^{-1}$ in the middle atmosphere are unrealistic; hence we present in Figure 6 our calculations which use as input the chemistry and parameter values that correspond to the PH model. In

particular, the PH model assumed $K = 5 \times 10^6 \text{ cm}^2 \text{ s}^{-1}$ and a nearly wet atmosphere. It is apparent from Figure 6, and the corresponding values listed in Table 3, that, only for the average water vapor mixing ratio of about 500 ppm, there is a near-balance between the CO_2 loss and production rates, which is consistent with the PH model (the PH model mentions only the necessity for a wet atmosphere, it does not specify the H_2O mixing ratio). Although the PH model does not include results for the various possible amounts of H_2O , our calculations in Figure 6 and Table 3 indicate that for the currently favored globally and seasonally averaged value of water vapor mixing ratio, about 150 ppm, the CO_2 recycling rate is smaller than its loss rate by a factor of about 3.

The MD and PH models were, however, based on laboratory data available nearly two decades ago. As discussed in the Photochemical Model section, two parameters in particular, the rate constant for reaction R9 (Table 1) which recycles CO_2 , and

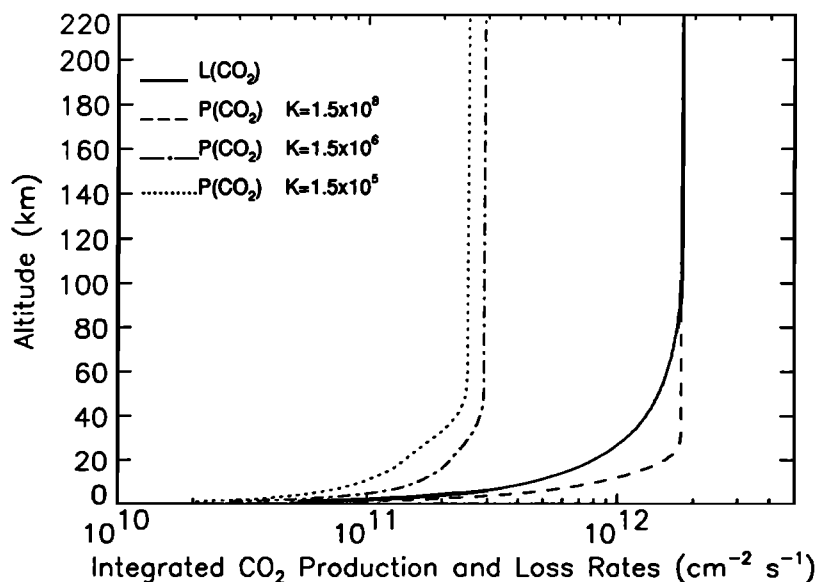


Figure 5. Production (P) and loss rates (L) of CO_2 for the MD model, but calculated for different values of eddy diffusion coefficient, K (in $\text{cm}^2 \text{ s}^{-1}$).

Table 2. Height-Integrated Production and Loss Rates of CO₂ and Their Ratios for the MD Model

	$K \text{ cm}^2 \text{ s}^{-1}$		
	1.50×10^5	1.50×10^6	1.50×10^8
$P_{\text{CO}_2} \text{ cm}^{-2} \text{ s}^{-1}$	0.25×10^{12}	0.29×10^{12}	1.70×10^{12}
$L_{\text{CO}_2} \text{ cm}^{-2} \text{ s}^{-1}$	1.80×10^{12}	1.80×10^{12}	1.80×10^{12}
$S_a = P_{\text{CO}_2}/L_{\text{CO}_2}$	0.14	0.16	0.94

Table 3. Height-Integrated Production and Loss rates of CO₂ and Their Ratios for the PH Model

	$\text{H}_2\text{O ppm}$		
	150	500	1000
$P_{\text{CO}_2} \text{ cm}^{-2} \text{ s}^{-1}$	0.58×10^{12}	1.87×10^{12}	2.58×10^{12}
$L_{\text{CO}_2} \text{ cm}^{-2} \text{ s}^{-1}$	1.80×10^{12}	1.80×10^{12}	1.80×10^{12}
$S_a = P_{\text{CO}_2}/L_{\text{CO}_2}$	0.32	1.04	1.43

the absorption cross section of CO₂ which directly controls the CO₂ loss rate, have been drastically revised since the above work was done. We have studied the effect of including the latest laboratory data for these two parameters on the MD model. With the exception of this change, and adopting a realistic value for $K = 10^6 \text{ cm}^2 \text{ s}^{-1}$ for the lower and middle atmosphere, the model parameters and chemistry remain the same as in the MD model. The resulting production and loss rates of CO₂ are shown in Figure 7. Whereas previously the production to loss ratio was 0.16 (for $K = 10^6$), now it is near unity. Thus, it might seem that a relatively simple change to the MD (or PH) model is all that is needed to explain the stability of the Martian atmosphere, except for the fact that there are other changes in the chemistry, input parameters, and the downward flux from the ionosphere. We will therefore now turn our attention to the results of our model with the latest chemical scheme and the input data (see Photochemical Model section for details of our model).

Our nominal model assumes $K = 10^6 \text{ cm}^2 \text{ s}^{-1}$ in the middle atmosphere and a profile of K as discussed in the previous section, $\text{H}_2\text{O} = 150 \text{ ppm}$ at the surface, and $\tau_d = 0.4$ in the vertical at the surface.

Figure 8 shows the distribution of hydrogen and oxygen species for the nominal model. Because of the emphasis in this paper on the production and loss rates of CO₂, which are mainly related to the lower atmosphere, the results are shown only to 80-km altitude. The calculations in the model, however, extend to 220 km, encompassing the ionosphere which provides a downward flux of carbon monoxide and oxygen produced in the ionosphere. The mixing ratios of O₂ and CO are initially fixed at their average values of 1.2×10^{-3} and 7×10^{-4} , respectively. In subsequent numerical iterations they are calculated as for any other constituents, and they are found to remain close to their initial values. This is not surprising considering the mixing time of these species is far smaller than their photochemical lifetimes.

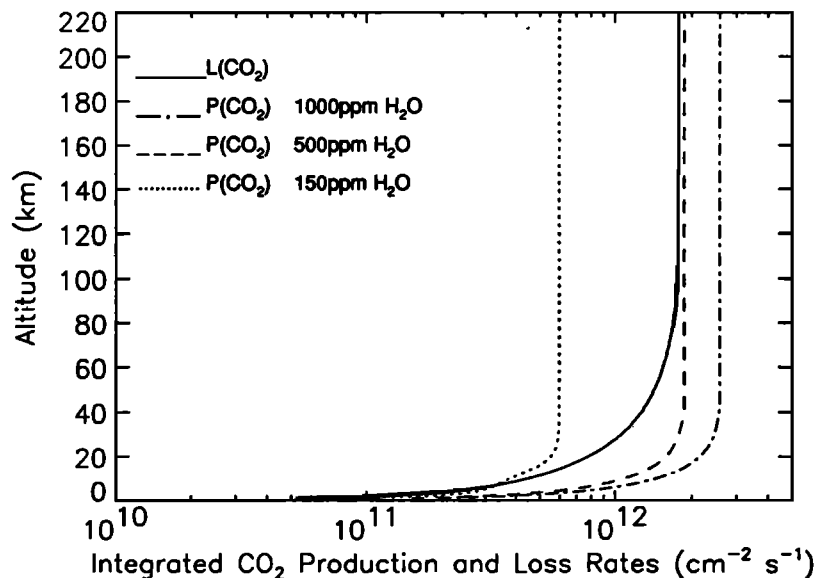


Figure 6. Production and loss rates of CO₂ for the PH model, but calculated for different values of water vapor mixing ratio.

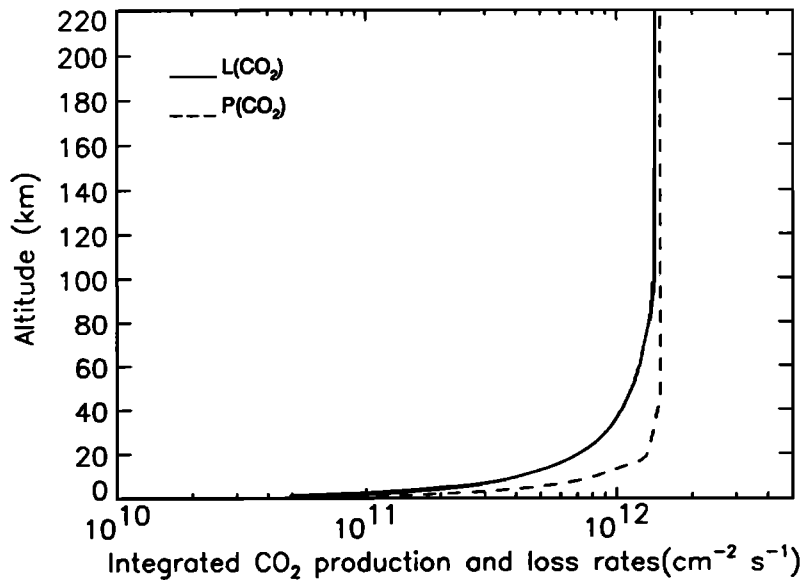


Figure 7. Production and loss rates of CO_2 , calculated using the MD chemical model and atmospheric parameters, except for new σ_{CO_2} , $k(\text{CO}+\text{OH})$, and $K (= 10^6 \text{ cm}^2 \text{ s}^{-1})$.

Of particular importance for the atmospheric stability question is the production of hydroxyl radical, OH. Therefore, we show schematically in Figure 9 the relative roles of the various sources of OH in the nominal model. The height-integrated production rates of OH are listed in Table 4a; their relative contributions are listed in Table 4b. Also listed in these tables are the values for the PH and MD models calculated using their chemistry and input parameters.

The production and loss rates of CO_2 for the nominal model ($K = 10^6 \text{ cm}^2 \text{ s}^{-1}$) are shown in Figure 10. The values of the height-integrated production and loss rates, P and L , and their ratio, the stability parameter, S_d , for the nominal model and for cases where $K = 10^5 \text{ cm}^2 \text{ s}^{-1}$ and $10^8 \text{ cm}^2 \text{ s}^{-1}$ are listed in Table 5. As expected, the photolysis loss rate is independent of the choice of K . Both Figure 10 and Table 5 indicate that the problem of recycling of CO_2 on Mars does not exist. On the contrary, it is

found that the production to loss ratio is always greater than one, no matter what value of the eddy diffusion coefficient in the lower and middle atmosphere is chosen. Only for $K \ll 10^5 \text{ cm}^2 \text{ s}^{-1}$ or $\gg 10^8 \text{ cm}^2 \text{ s}^{-1}$ we find a significant departure from this conclusion. However, production rate of CO_2 which is greater than its loss rate is clearly a physically unrealistic situation that calls for a process which may have been overlooked or not yet properly included in the model. In the following section we discuss various possibilities which could allow the Martian atmosphere to maintain complete stability.

Discussion

Before resorting to some new process to balance the production and loss rates of CO_2 on Mars, we first examine the impact of changing certain input parameters, either because they have

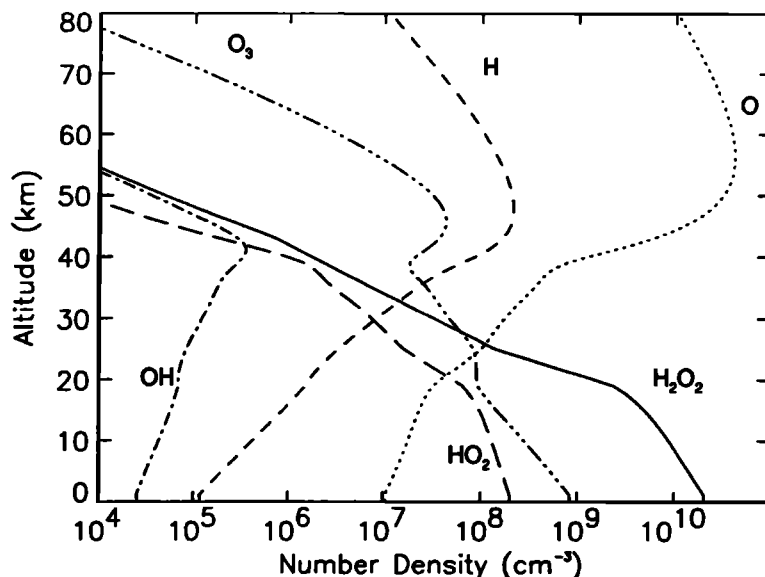


Figure 8. Distribution of key constituents based on the nominal model ($\text{H}_2\text{O} = 150 \text{ ppm}$, $K = 10^6 \text{ cm}^2 \text{ s}^{-1}$, $\tau_d = 0.4$; see text).

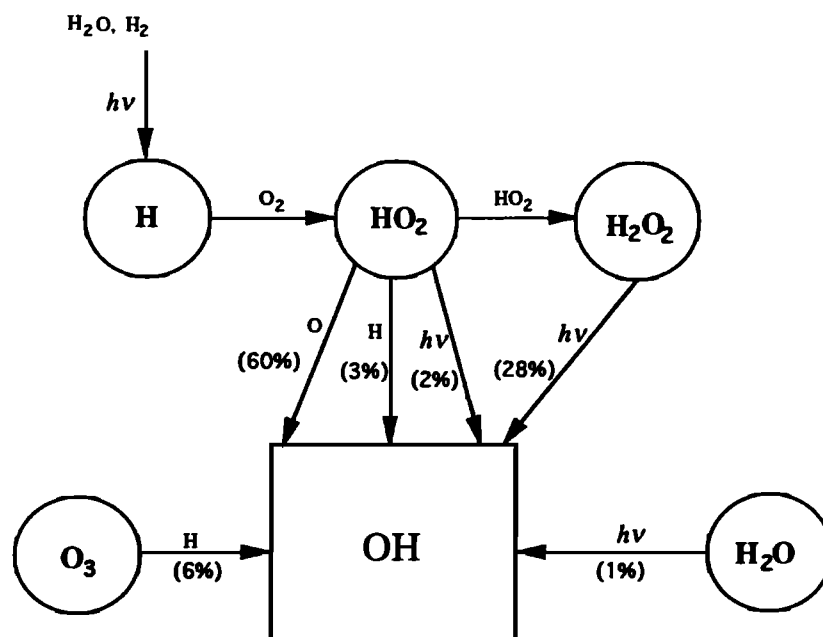


Figure 9. Schematic showing the relative contributions of the various sources to the OH production rate in the nominal model.

uncertainties or known variations. In particular, we discuss the sensitivity of the results to changes in the atmospheric dust content, inclusion of nitrogen chemistry, uncertainty in the absorption cross sections of water vapor, and the variation of the atmospheric water vapor content.

The optical depth of dust on Mars can have large variations, as discussed earlier. In the nominal model discussed above, a globally and seasonally averaged vertical optical depth in the ultraviolet, $\tau_d = 0.4$ at ground was taken. In Figure 11 we give the CO_2 production and loss rates for $\tau_d = 0$ and 2.0, representing a fairly typical extreme. Table 6 lists the CO_2 production and loss rates for $\tau_d = 0, 0.4, 1.0$ and 2.0. From Figure 11 and Table 6, one can conclude that the stability parameter, S_a is not affected dramatically unless the dust optical depth exceeds unity. This result is for the case where $K = 10^6 \text{ cm}^2 \text{ s}^{-1}$ in the lower and middle atmosphere, and H_2O is 150 ppm. The direct consequence of

the increased dust opacity is a reduction in the solar flux which will in turn reduce the photolysis rates of CO_2 and H_2O , in particular. The change in the height integrated values, however, is small. For instance, the CO_2 photolysis rate decreases by only 15% when the dust opacity is increased from 0 to 2. Thus, the optical depth of dust alone is not expected to be a controlling factor in determining the stability of the Martian atmosphere, since $\tau_d > 1$ cannot be considered to represent mean conditions on Mars. It should be stressed, however, that the horizontal and vertical distributions of the atmospheric constituents would be affected by changes in the dust opacity, either directly or indirectly.

The nominal model of this paper neglected reactions involving any form of nitrogen. The following reaction, in particular, can be an additional source of hydroxyl radicals:

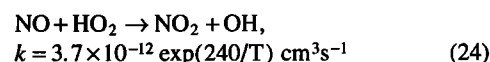


Table 4a. Height-Integrated Production Rates of OH (in $\text{cm}^{-2} \text{ s}^{-1}$) From Different Sources for the MD, PH and the Present Models

	$\text{HO}_2 + \text{O}$	$J(\text{H}_2\text{O}_2)$	$J(\text{H}_2\text{O})$	$\text{O}_3 + \text{H}$	$\text{HO}_2 + \text{H}$	$J(\text{HO}_2)$
MD	0.17×10^{13}	0.38×10^{10}	0.77×10^9	0.25×10^{12}	0	0
PH	0.17×10^{13}	0.13×10^{13}	0.46×10^{11}	0.96×10^{11}	0.66×10^{11}	0.98×10^{11}
Present	0.72×10^{12}	0.33×10^{12}	0.91×10^{10}	0.66×10^{11}	0.40×10^{11}	0.23×10^{11}

Table 4b. Relative Contributions of the Various Sources to the OH Production Rates for the MD, PH and the Present Models

	$\text{HO}_2 + \text{O}$	$J(\text{H}_2\text{O}_2)$	$J(\text{H}_2\text{O})$	$\text{O}_3 + \text{H}$	$\text{HO}_2 + \text{H}$	$J(\text{HO}_2)$
MD	87.0	0.2	0	12.8	0	0
PH	51.4	39.3	1.4	2.9	2.0	3.0
Present	60.6	27.8	0.8	5.5	3.4	1.9

Values are in percent.

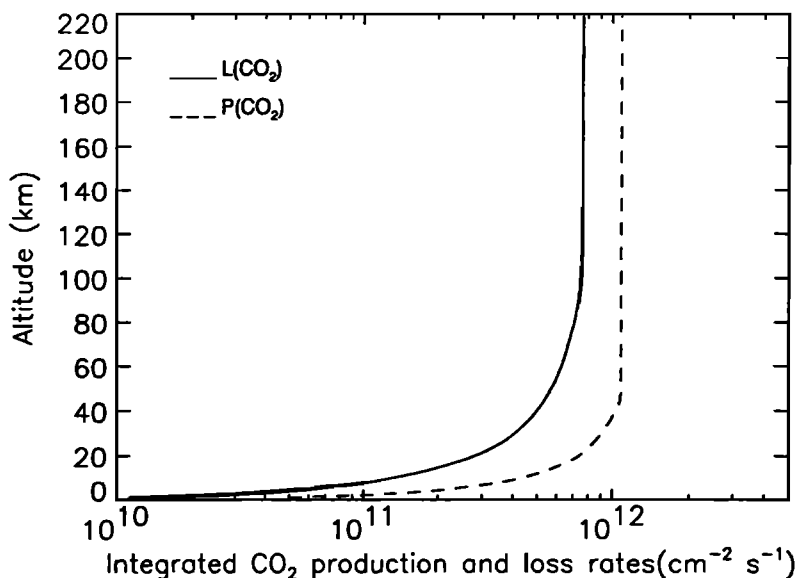


Figure 10. Production and loss rates of CO_2 for the nominal model.

However, we find that inclusion of above reaction and other less important nitrogen reactions has virtually no impact on the atmospheric levels of CO_2 , CO and O_2 ; only the H_2 mole fraction is reduced slightly.

As mentioned in the Photochemical Model section, there is some uncertainty associated with the H_2O absorption cross sections, $\sigma_{\text{H}_2\text{O}}$, especially with regard to their temperature dependence. Since the measured H_2O cross sections are at room temperature (298 K) and the Martian temperature in the relevant altitude range is closer to 200 K, we study the effect of reducing the $\sigma_{\text{H}_2\text{O}}$ by a factor of 2 and 3 on the CO_2 recycling rate (which is directly related to the OH density), assuming that the temperature dependence of $\sigma_{\text{H}_2\text{O}}$ is similar to that of the CO_2 absorption cross sections. The result, along with a comparison of the case with $\sigma_{\text{H}_2\text{O}}$ at room temperature, is shown in Figure 12 and the corresponding values are listed in Table 7. The CO_2 photolysis rate is not affected significantly, as expected; the CO_2 production rate, on the other hand, changes somewhat. As we note in Table 7, the ratio of CO_2 production to loss rate with $\sigma_{\text{H}_2\text{O}}$ reduced by a factor of 2 and 3, e.g., decreases to 1.3 and 1.2, respectively, from a value of 1.4 which corresponds to $\sigma_{\text{H}_2\text{O}}$ at room temperature; all other input parameters being the same. Although, within the range of reduction in $\sigma_{\text{H}_2\text{O}}$ considered here, there is little change in the stability parameter, S_a , this sensitivity study demonstrates the importance of accurate laboratory measurements. If it should turn out that these cross sections have a temperature dependence more acute than that of CO_2 cross sections, the problem of stability of CO_2 in the Martian atmosphere may not be that serious. Note, however, that the measurement of

$\sigma_{\text{H}_2\text{O}}$ is challenging at low temperatures because of the low saturation vapor pressure of water vapor, which is, for example, only 1.2×10^{-3} mmHg at 200 K and 1.5×10^{-5} mmHg at 175 K.

Finally, the water vapor amount in the atmosphere of Mars shows a large temporal, latitudinal and longitudinal variation, ranging from a nearly dry atmosphere (≤ 1 pr μm) to a nearly wet atmosphere (≥ 60 pr μm). The nominal model in this paper assumes a globally and seasonally averaged value of 10 pr μm H_2O at the surface. Our calculations for the nominal model, but using $\text{H}_2\text{O} = 1$ ppm (dry) yield a value of the stability parameter, $S_a = 0.9$, and $S_a = 1.9$ if $\text{H}_2\text{O} = 1000$ ppm (wet). In the nominal model, with $\text{H}_2\text{O} = 150$ ppm, S_a was 1.4. Water vapor amounts exceeding the average value give values of S_a greater than 1.4, reaching a plateau with H_2O around 30 pr μm (~ 500 ppm) at the surface, since greater amounts of water vapor at the surface do not generally result in greater water vapor mixing ratio throughout the atmosphere because of saturation. This sensitivity study illustrates that the amount of water vapor on Mars can exert a significant control over the recycling rate of CO_2 locally. The nominal model of this paper, which is based on an average water vapor amount, is, however, still representative of the globally and seasonally averaged conditions, as far as the stability of the atmosphere is concerned.

Conclusion

The above discussion on the sensitivity of CO_2 recycling rate to the known and suspected variations in the atmospheric and laboratory parameters indicates that according to the present

Table 5. Height-Integrated Production and Loss Rates of CO_2 and Their Ratios for the Present Model With Different Values of K in the Middle Atmosphere

	$K \text{ cm}^2 \text{ s}^{-1}$		
	10^5	10^6	10^8
$P_{\text{CO}_2}, \text{cm}^{-2} \text{ s}^{-1}$	1.08×10^{12}	1.08×10^{12}	1.17×10^{12}
$L_{\text{CO}_2}, \text{cm}^{-2} \text{ s}^{-1}$	0.77×10^{12}	0.77×10^{12}	0.77×10^{12}
$S_a = P_{\text{CO}_2} / L_{\text{CO}_2}$	1.40	1.40	1.52

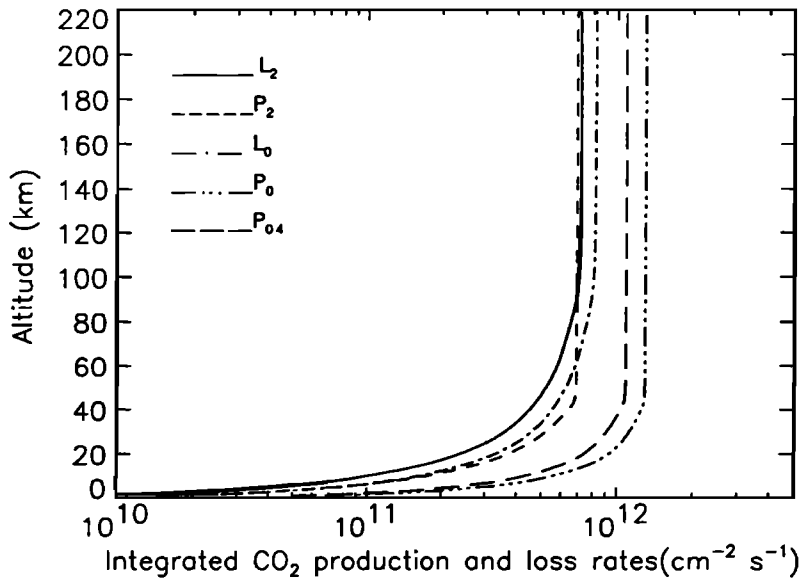


Figure 11. Production and loss rates of CO₂ for the nominal model, except that τ_d is taken to be 0 and 2 here. A comparison with the nominal model, with $\tau_d = 0.4$, is also shown for CO₂ production rate only; the photolysis loss rate for this model is not plotted here to avoid crowding, but is shown in Figure 10. Subscripts in the figure legends denote the value of τ_d .

Table 6. Sensitivity of the Height-Integrated Production and Loss Rates of CO₂ and the Stability Parameter, S_a , to the Dust Optical Depth

	τ_d			
	0	0.4	1	2
P_{CO_2} cm ⁻² s ⁻¹	1.29×10^{12}	1.08×10^{12}	0.86×10^{12}	0.69×10^{12}
L_{CO_2} cm ⁻² s ⁻¹	0.82×10^{12}	0.77×10^{12}	0.73×10^{12}	0.71×10^{12}
$S_a = P_{CO_2}/L_{CO_2}$	1.57	1.40	1.18	0.97

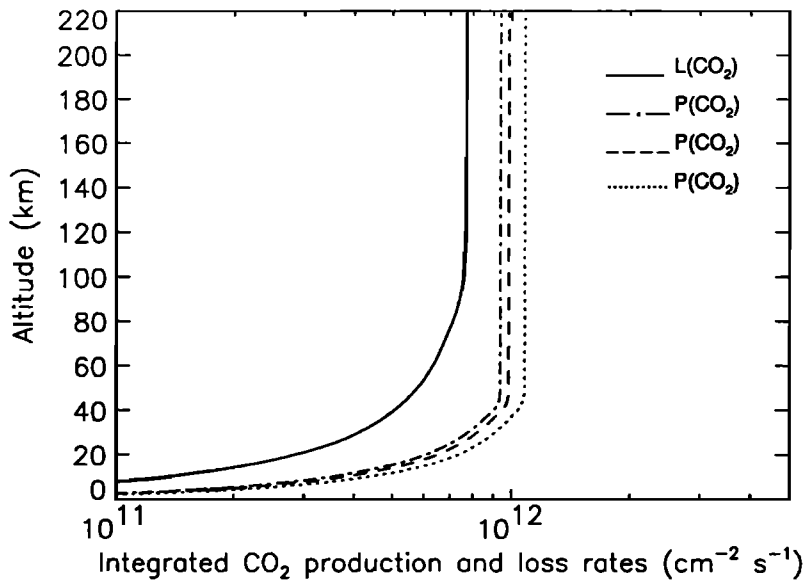


Figure 12. Production and loss rates of CO₂ for the nominal model, except that water vapor absorption cross sections here are reduced by a factor of 2 (dashed line) and 3 (dash-dotted line). A comparison with σ_{H_2O} at room temperature (dotted line) is also shown.

Table 7. Sensitivity of the Height-Integrated Production and Loss Rates of CO₂ and the Stability Parameter, S_a , to the Water Vapor Absorption Cross Section

	$\sigma_{\text{H}_2\text{O}}$	$(1/2)\sigma_{\text{H}_2\text{O}}$	$(1/3)\sigma_{\text{H}_2\text{O}}$
P_{CO_2} cm ⁻² s ⁻¹	1.08×10^{12}	0.99×10^{12}	0.94×10^{12}
L_{CO_2} cm ⁻² s ⁻¹	0.77×10^{12}	0.77×10^{12}	0.77×10^{12}
$S_a = P_{\text{CO}_2}/L_{\text{CO}_2}$	1.40	1.29	1.22

photochemical model for globally and seasonally averaged conditions, there is an imbalance between the production and loss rates of CO₂, with production rate exceeding the loss rate by about 40%. This implies that the recycling rate of carbon dioxide on Mars needs to be throttled down. Our homogeneous gas phase photochemical model of this paper does not provide an effective mechanism for doing this. It is, however, possible that the atmospheric aerosols, especially dust particles, could provide surfaces on which water vapor, H₂O₂, OH, O or CO could be adsorbed. Anbar *et al.* [1993b] and H. Nair *et al.* (A photochemical model of the Martian atmosphere, submitted to *Icarus*, 1994) have also suggested the importance of aerosol sink for HO_x. Such a sink to the species that play a central role in the recycling of CO₂ on Mars will have the effect of reducing the CO₂ production rate, perhaps even to the level of its photolysis loss rate. This process may, in fact, be a blessing in disguise, as the earlier suggestion for increasing the CO₂ recycling rate does not seem to be borne out by laboratory data on the accommodation coefficients, although all of them are not yet measured. We conclude therefore that heterogeneous processes in the atmosphere of Mars could be potentially important in providing a sink to certain species, such as H₂O, H₂O₂, OH, CO or O, and thereby maintaining stability of the atmosphere.

The one-dimensional model of this paper represents only a preliminary attempt at addressing the classical question of the stability of Martian atmosphere. It is nonetheless an important step since it provides the framework for developing more complex models, and it identifies the laboratory and planetary information critically needed to adequately model the problem. We have begun the formulation of a two-dimensional model, and with the help of a general circulation model sometime in the future, we expect to have a more complete model of the stability of species in the atmosphere of Mars. It is hoped that high-resolution data on the temporal and spatial distributions of atmospheric constituents, particularly aerosols of dust and ice, water vapor, hydroxyl, hydrogen peroxide, oxygen, ozone and carbon monoxide, as well as the mineralogy of dust, will become available from future observations. At the same time we urge our laboratory colleagues to take up the challenge of measuring the relevant accommodation coefficients, rate constants and the absorption cross sections appropriate for the Martian environmental and surface conditions. It is only after these efforts that one can fully evaluate whether a heterogeneous process needs to be invoked to maintain stable levels of CO₂, CO and O₂ in the atmosphere of Mars.

Acknowledgment. We thank T.M. Donahue, D.M. Hunten, C. Sagan, M. Allen and A.D. Anbar for their valuable comments on this work. This research was supported by grants NAGW-2561 and NAGW-1771 from the Solar System Exploration Division of the National Aeronautics and Space Administration.

References

- Anbar, A.D., M. Allen, and H.A. Nair, Photodissociation in the atmosphere of Mars: Impact of high resolution, temperature-dependent CO₂ cross section measurements, *J. Geophys. Res.*, **98**, 10,925-10,931, 1993a.
- Anbar, A.D., M.T. Leu, H.A. Nair, and Y.L. Yung, Adsorption of HO_x on aerosol surfaces: Implications for the atmosphere of Mars, *J. Geophys. Res.*, **98**, 10,933-10,940, 1993b.
- Atkinson, R., D.L. Baulch, R.A. Cox, R.F. Hampson Jr., J.A. Kerr, and J. Troe, Evaluated kinetic and photochemical data for atmospheric chemistry, Supplement 3, *J. Phys. Chem. Ref.*, **18**, 881-1097, 1989.
- Atreya, S.K., and J.E. Blamont, Stability of the Martian atmosphere: Possible role of heterogeneous chemistry, *Geophys. Res. Lett.*, **17**, 287-290, 1990.
- Banks, P.M., and G. Kockarts, *Aeronomy*, pp. 38-41, Academic, San Diego, Calif., 1973.
- Chassefiere, E., J.E. Blamont, V.A. Krasnopolsky, O.I. Korablev, S.K. Atreya, and R.A. West, Vertical structure and size distributions of Martian aerosols from solar occultation measurements, *Icarus*, **97**, 46-69, 1992.
- DeMore, W.B., C.J. Howard, S.P. Sander, A.R. Ravishankara, D.M. Golden, C.E. Kolb, R.F. Hampson, M.J. Molina, and M. J. Kurylo, Chemical kinetics and photochemical data for use in stratospheric modeling, *JPL Publ.*, 92-20, 1992.
- Drossart, P., J. Rosenqvist, S. Erard, Y. Langevin, B.J.P. Ibring, and M. Combes, Martian aerosol properties from the Phobos/ISM experiment, *Ann. Geophys.-Atmos. Hydrospheres Space Sci.*, **9**, 11,754-11,761, 1991.
- Farmer, C.B., D.W. Davis, A.L. Holland, D.D. La Porte, and P.E. Docus, Water vapor observations from the Viking orbiters, *J. Geophys. Res.*, **82**, 4225-4248, 1977.
- Gericke, K.H., and F.J. Comes, Energy partitioning in the reaction O(¹D) + H₂O → OH + OH: The influence of O(¹D) translational energy on the reaction rate constant, *Chem. Phys. Lett.*, **81**, 218-221, 1981.
- Hedde, D.W.O., Photon scattering processes, *J. Quant. Spectrosc., Radiat. Transfer*, **2**, 349-357, 1962.
- Hudson, R.D., and L.J. Kieffer, Absorption cross sections of stratospheric molecules, in *The Natural Stratosphere of 1974, Clim. Impact Assessment Program Monogr.*, vol.1, pp. 5-156, U.S. Dept. of Transportation, Arlington, Virginia, 1975.
- Hunten, D.M., Vertical transport in atmosphere, in *Atmosphere of Earth and Planets*, edited by B.M. McCormac, pp. 59-72, D. Reidel, Norwell, Mass., 1975.
- Jakosky, B.M., and C.B. Farmer, Seasonal and global behavior of water vapor in the Mars atmosphere, *J. Geophys. Res.*, **87**, 2999-3019, 1982.
- Kahn, R., Ice haze and snow and the Mars water cycle, *J. Geophys. Res.*, **95**, 14,677-14,693, 1990.
- Keyser, L.F., Kinetics of the reaction OH + HO₂ → H₂O + O₂ from 254 to 382 K, *J. Phys. Chem.*, **92**, 1193-1200, 1988.
- Kong, T.Y., and M.B. McElroy, Photochemistry of the Martian atmosphere, *Icarus*, **32**, 168-189, 1977.
- Korablev, O.I., V.A. Krasnopolsky, and A.V. Rodin, Vertical structure of Martian dust measured by the solar infrared occultations from Phobos spacecraft, *Icarus*, **102**, 76-87, 1991.

- Krasnopolsky, V.A., *Photochemistry of the Atmospheres of Mars and Venus*, pp. 87, Springer-Verlag, New York, 1986.
- Krasnopolsky, V.A., Photochemistry of the Martian Atmosphere (mean conditions), *Icarus*, 101, 313-332, 1993.
- Larson, C.W., P.H. Stewart, and D.M. Golden, Pressure and temperature dependence of reactions proceeding via a bound complex. An approach for combustion and atmospheric chemistry modelers, *Int. J. Chem. Kinet.*, 20, 27-40, 1988.
- Leu, M.T., J.E. Blamont, A.D. Anbar, L.F. Keyser, and S.P. Sander, Adsorption of CO on oxide water ice surfaces: Implications for the Martian atmosphere, *J. Geophys. Res.*, 97, 2621-2627, 1992.
- Lewis, B.R., and J.H. Carver, Temperature dependence of the carbon dioxide photoabsorption cross section between 1200 and 1970 A, *J. Quant. Spectrosc. Radiat. Transfer*, 30, 297-309, 1983.
- Lindzen R.S., Turbulence and stress owing to gravity wave and tidal breakdown, *J. Geophys. Res.*, 86, 9707-9714, 1981.
- Lindzen, R.S., Tides and gravity waves in the upper atmosphere, in *Mesospheric Models and Related Experiments* edited by G. Fiocco, pp. 122-130, D. Reidel, Norwell, Mass., 1971.
- McElroy, M.B., and T.M. Donahue, Stability of the Martian atmosphere, *Science*, 177, 986-989, 1972.
- Mount, G.H., and G.J. Rottman, The solar absolute spectral irradiance 1150-3173 A: May 17, 1982, *J. Geophys. Res.*, 88, 5403-5410, 1983.
- Nier, A.O., and M.B. McElroy, Composition and structure of Mars' upper atmosphere: Results from the neutral mass spectrometers on Viking 1 and 2, *J. Geophys. Res.*, 82, 4341-4349, 1977.
- Okabe, H., *Photochemistry of Small Molecules*, pp. 264 and 282, John Wiley, New York, 1978.
- Parkinson, T.D., and D.M. Hunten, Spectroscopy and aeronomy of O₂ on Mars, *J. Atmos. Sci.*, 29, 1380-1390, 1972.
- Press, W.H., B.P. Flannery, S.A. Teukolsky, and W.T. Vetterling, *Numerical Recipes*, pp. 269-272, Cambridge University Press, New York, 1989.
- Seiff, A., Post-Viking models for the structure of the summer atmosphere of Mars, *Adv. Space Res.*, 2, (2), 3-18, 1982.
- Shemansky, D.E., CO₂ extinction coefficient 1700-3000 A, *J. Chem. Phys.*, 56, 1582-1587, 1972.
- Shi, J., and R. Barker, Kinetics studies of the reactivation of O₂(¹Σ_g⁺) and O(¹D), *Int. J. Chem. Kinet.*, 20, 1283-1301, 1990.
- Slanger, T.G., R.J. Wood, and G. Black, Kinetics of O(³P) + CO + M recombination, *J. Chem. Phys.*, 57, 233-238, 1972.
- Thevenet, A., F. Juillet, and S.J. Teichner, Photointeraction on the surface of titanium dioxide between oxygen and carbon monoxide, *Jpn. J. Appl. Phys. Suppl. 2*, Pt. 2, 529-532, 1974.
- Thompson, B.A., P. Harteck, and R.R. Reeves Jr., Ultraviolet absorption coefficients of CO₂, CO, O₂, H₂O, N₂O, NH₃, NO, SO₂, and CH₄ between 1850 and 4000 A, *J. Geophys. Res.*, 68, 6431-6436, 1963.
- Tsang, W., and R.F. Hampson, Chemical kinetic data base for combustion chemistry, Part 1, Methane and related compounds, *J. Phys. Chem. Ref.*, 15, 1087-1279, 1986.
- Washburn, E.W., The vapor pressure of ice and of water below the freezing point, *Mon. Weather Rev.*, 52, 488-490, 1924.
- Watanabe, K., E.C.Y. Inn, and M. Zelikoff, Absorption coefficients of oxygen in the vacuum ultraviolet, *J. Chem. Phys.*, 21, 1026-1030, 1953.
- World Meteorological Organization, (WMO), Geneva, Atmospheric ozone, Rep. 16, Global Ozone Research and Monitoring Project Report, 1985.
- Zurek, R.W., Martian great dust storms: An update, *Icarus*, 50, 288-310, 1982.
-
- S.K. Atreya, Department of Atmospheric, Oceanic and Space Sciences, Space Research Bldg., University of Michigan, Ann Arbor, MI 48109-2143. (email: sushil_atreya@um.cc.umich.edu)
- Z.G. Gu, Department of Atmospheric, Oceanic and Space Sciences, University of Michigan, Ann Arbor, MI 48109-2143. (email: zhen@engin.umich.edu)

(Received October 27, 1993; revised April 14, 1994; accepted April 21, 1994.)